Journal of Advance Engineering Research
ISSN: 2393-8447
Volume 8, Issue 1, pp.71-76

Design and Analysis of Contactless Support in Multi-Channel Cryoline using Magnetic Levitation

Sandeep Kumar Shah[1,*], Dr R G Kapadia[1], R O Paliwal[1]

[1]Department of Cryogenics Engineering, L D College of Engineering, Ahmedabad-380015, Gujarat, India

*Corresponding author email: shahsandeep1998@gmail.com,

ABSTRACT

Conduction and radiation are two significant sources of heat loss in vacuum jacketed cryogenic transfer lines. Radiation because of a temperature difference between a warm outer pipe and a cold inner pipe and conduction because of the heat transfer through supports. The fixed supports are the necessary part as it provides the vacuum enclosure within the cryoline. But the sliding support, used to carry the weight of the section of pipe to prevent the bending of pipe, can be replaced with a magnetic levitation system to minimize the conduction heat loss in the cryoline. Support with a magnetic levitation system is designed here to replace conventional sliding supports. Utilization of Halbach arrays of the $Nd_2Fe_{14}B$ (N42) and Ceramic magnets (grade 8) to perform the levitation. For the levitation of the process pipes, about 6.7×10^5 N/m^3 force density is required. The numerical simulation is done using the Solidworks EMS tool.

Keywords – Cryogenic Transfer Line, Supporting Structure, Heat loss prevention, Halbach arrays, Magnetic Levitation

1. INTRODUCTION

Widespread users of cryogenic transfer lines in many extensive scientific facilities of cryogenic transfer lines are cryomodules with superconducting cavities and cryostats with superconducting magnets, bus bars, or cryogenic vacuum pumps. [1] They need cryogens at very low and a variety of temperatures. Fig. *1* depicts the example; the cryogenic plant supplies supercritical helium at a temperature of 4.5 K from cryogenic plant to cryogenic device by He supply line. Then, gaseous helium returns at nearly 5 K by vapor low-pressure return line (VLP return). Similarly, another circuit of transfer line transferring He at 40-80 K by thermal shield circuit containing TS supply and return lines.

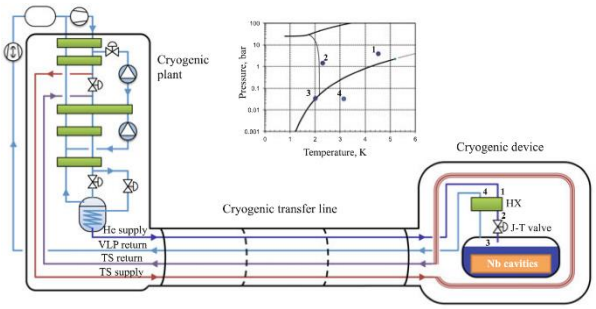

Fig. 1 Schematic of an example of cryogenic system having complex transfer line [1]

In their paper, P. Duda et al. [2] conducted a case study on the design and thermodynamic performance analysis of a multi-channel cryogenic transfer line for XFEL AMTF. The plan of XATL1 includes the internal structure, which consists of four process pipes, i.e., Supercritical Helium supply, Gaseous Helium Return lines, and Thermal Shield supply, and return lines, as shown in Fig. *2*. The analysis was performed based on the 2nd law of thermodynamics by calculating the entropy generated in the entire cryoline. In this paper, they concluded that to compensate for the

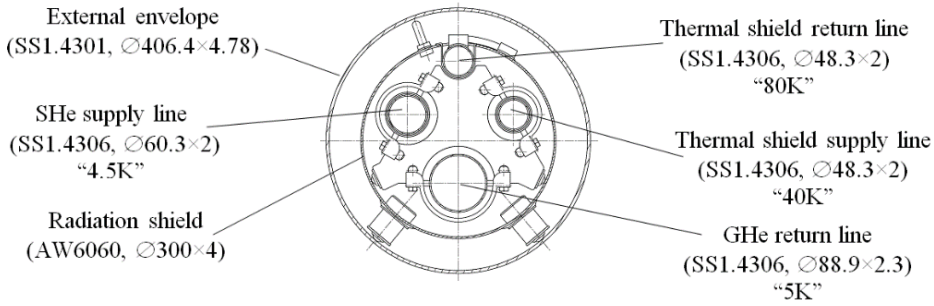

Fig. 2 Cross-section of the cryogenic transfer line XATL1 [2]

irreversibilities caused by the heat losses, 4.11 kW of energy is required. Thermodynamic analysis of support and multi-layer insulation of simple transfer lines is carried out by B. C. Deng et al. [3]. The heat inleaks in 2 m simple pipe in vacuum jacket cryoline with two supports are shown in Table 1.

Table 1: Heat inleak in simple cryoline [3]

Structure	Simulation Q (W)			Experiment Q (W)		
	Q_s	Q_i	Q_t	Q_s	Q_i	Q_t
Triangular support	0.488	0.911	1.359	0.435	1.020	1.455
Three-plate support	0.279	0.766	1.045	0.310	0.735	1.046
Two-plate support	0.205	0.733	0.938	0.200	0.735	0.935

Magnetic levitation or magnetic suspension is a technique by which a magnetic object is levitated with no support other than magnetic fields. [4] So, the direct contact between the process pipe and vacuum jacket in simple cryoline and all process pipes and the radiation shield in multi-channel cryoline can be eliminated using the magnetic levitation system. For successful levitation, it is necessary to counterbalance the gravitational force on the object by magnetic force, i.e., $\vec{F}_{magnetic} + \vec{F}_{gravity} = 0$. [5] $\vec{F}_{magnetic}$ is given by **(1)** and $\vec{F}_{gravity}$ is provided by **(2)**.

$$\vec{F}_{magnetic} = \frac{\Delta\chi V}{2\mu_0}(\vec{B}.\nabla)\vec{B} \qquad \textbf{(1)}$$

$$\vec{F}_{gravity} = \rho\vec{g}V \qquad \textbf{(2)}$$

A Halbach array can enhance and concentrate the magnetic field as per the requirement to improve the levitation system. [6]

Superconductors are perfectly diamagnetic, thanks to the Meissner effect. A magnetic field's expulsion is encountered during the superconductor transition to the superconducting state when it is cooled below the critical temperature. [7] When liquid cryogen flows from the process pipe, it will inherently generate the perfect condition to achieve superconductivity. But when the cryogenic line is in an ideal situation, i.e., at room temperature, it needs warm support to lift the weight of the process pipe. So, in such a case, an arrangement will be necessary for that situation. In the case of multi-channel cryoline, the complexity of the design will be significantly increased. So, this method is not tried in this study.

2. MAGNETOSTATIC

A permanent magnet is a material that will begin to exhibit a magnetic field of its own when inserted into a strong magnetic field. [8] Indeed, the exhibited magnetic field would allow the magnet to exert force, i.e., the ability to attract or repel, on other magnetic materials. Such exhibited magnetic field would then be continuous without weakening, provided the material is not subjected to a change in temperature, demagnetizing field, etc. However, at low temperatures, the magnetic properties of the magnet become stronger. This type of material is characterized by a B-H Curve that starts in the second quadrant if it exhibits nonlinear behavior. From the B-H curve, the Remanence, B_R, and Coercivity, H_c can be known.

Magnetostatic or the so-called DC Magnetic Field analysis belongs to the low-frequency electromagnetic domain or regime; i.e., displacement currents are neglected. In addition, the fields depend on position only. They do not depend on time. Furthermore, the size of the object is much smaller than the wavelength. The Magnetostatic Analysis calculates the magnetic fields produced by a permanent magnet. It utilizes Maxwell's equation to calculate the magnetic field and the magnetic force. [9]

$$\nabla \times H = J_s \qquad \textbf{(3)}$$

$$\nabla \cdot B = 0 \qquad \textbf{(4)}$$

Where H is the magnetic field, J_S is the current source density, and B is the magnetic flux density. Thus, the constitutive relation connects B and H as shown in **(5)**.

$$B = \mu(H + H_c) \qquad \textbf{(5)}$$

Where, μ is magnetic permeability, in general, a function of $H \cdot H_c$ is the Coercivity. Thus, these are the equations solved by magnetostatic simulation. In software, the value of H and B_R is already given. We only need to define the direction of Coercivity.

3. DESIGNING AND PREPARING SIMULATION BACKGROUND

Two concentric magnetic rings can be utilized to isolate the process pipe from unwanted thermal contact, provided both concentric magnetic rings should repel each other with a force of repulsion greater than the gravitational force. Two Halbach arrays of magnets are utilized to enhance the magnetic field in the annular space of concentric magnetic rings. Fig. *4* and Fig. *3* show the arrangement of arrays that can gather the magnetic field lines in the annular space so that they will oppose each other. The head shows the north pole, and the tail indicates the south pole of the magnet.

The design of the magnetic levitation system of the multi-channel cryoline is done based on the dimension shown in Fig. *2*. Fig. *5* depicts the design of the sliding support with a magnetic levitation system for the multi-channel cryogenic transfer line. The details of the component selected for the design are shown in Table 2. All magnets are 30 mm thick. Two different magnetic materials are chosen for the levitation system, i.e., $Nd_2Fe_{14}B$ magnet (N42) and Ceramic magnet (grade 8). The Remanence, Coercivity, and relative permeability are 1.35 T, 891268 A/m, and 1.1205 for $Nd_2Fe_{14}B$ magnet (N42), and 0.39 T, 254648 A/m, and 1.2187 for Ceramic magnet (grade 8), respectively. The modification is done only in support of the multi-channel cryoline so, only 1 m of cryoline is modeled, which contains the support with a magnetic levitation system employing Solidworks. The required force density for the levitation can be calculated using **(2)**. An average of 6.7×105 N/m^3 of force density is needed for the levitation of each line considering at every 5 m length; one sliding support is provided to prevent the bending of the pipe.

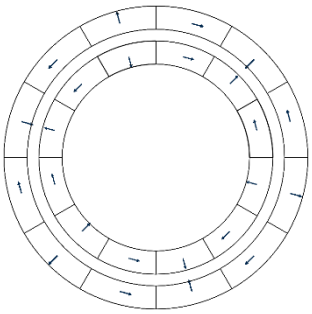

Fig. 4 Magnetic array 1

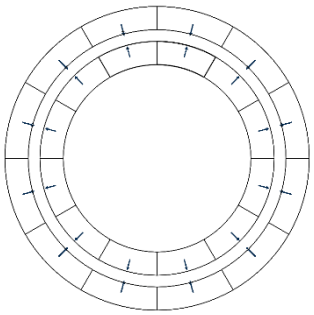

Fig. 3 Magnetic array 2

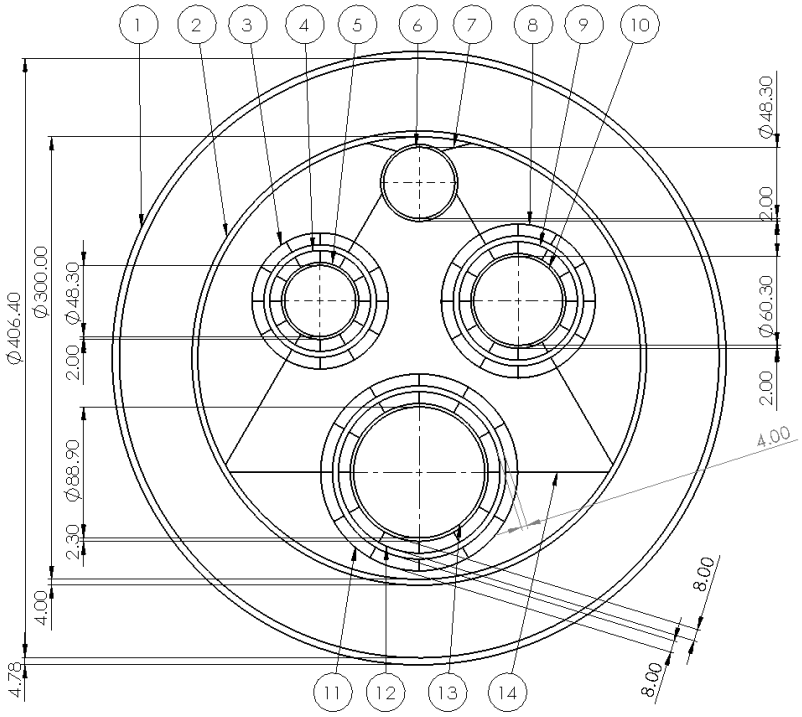

Fig. 5 Dimension of Cryogenic transfer line with magnetic levitation system

Table 2: Component details of the multi-channel cryoline

No.	Component name	Dimension(mm)	Mass	Material
1.	External envelope	Ø406.40×4.78	49.39(kg/m)	SS1.4301
2.	Radiation shield	Ø300×4	10.31(kg/m)	AW6060
3.	Thermal shield supply line magnet out	Ø76.30×8	63.53(g/sup)	N42 and ceramic magnet grade 8
4.	Thermal shield supply line magnet in	Ø52.30×8	45.47(g/sup)	N42 and ceramic magnet grade 8
5.	Thermal shield supply line	Ø48.30×2	2.53(kg/m)	SS1.4306
6.	Thermal Shield return line	Ø48.30×2	2.53(kg/m)	SS1.4306
7.	Copper thermal link	5 mm thick	101.86(g/sup)	Copper
8.	Supercritical Helium supply line magnet out	Ø88.30×8	544.56(g/sup)	N42 and ceramic magnet grade 8
9.	Supercritical Helium supply line magnet in	Ø64.30×8	408.85(g/sup)	N42 and ceramic magnet grade 8
10.	Supercritical Helium supply line	Ø60.30×2	3.13(kg/m)	SS1.4306
11.	Gaseous Helium return line magnet out	Ø117.50×8	709.69(g/sup)	N42 and ceramic magnet grade 8
12.	Gaseous Helium return line magnet out	Ø93.50×8	573.97(g/sup)	N42 and ceramic magnet grade 8
13.	Gaseous He return line	Ø88.90×2.30	5.27(kg/m)	SS1.4306
14.	Support	30 mm thick	797.95(g)	G-10 glass epoxy

4. SIMULATION RESULTS

The simulation of the modified model is done four times with two different materials and with each material having two different configurations. The results are as follows:

4.1 For N42 Magnet and Magnetic Array 1

Fig. *6* and Fig. *7* show the proposed model's magnetic flux density and force density with a $Nd_2Fe_{14}B$ magnet (N42) as the material having magnetic array 1 configuration. The average magnetic flux density and force density is about 5.63×10^{-1} T and 1.12×10^{8} N/m^3, respectively. Here, it can be seen that there are three focus points where the flux density is highest in the annular gap between the magnetic arrays. The vector direction in between the annular space is colliding with each other, which confirms the levitation.

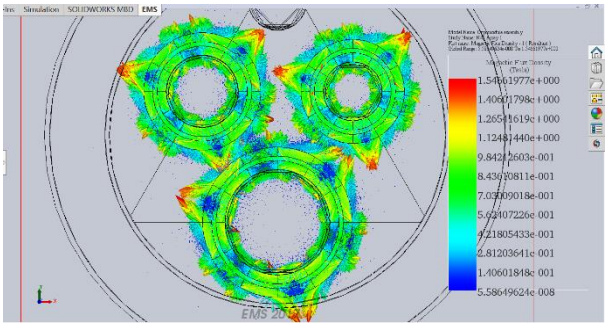

Fig. 6 Magnetic flux density for Nd2Fe14B magnet (N42) and magnetic array 1

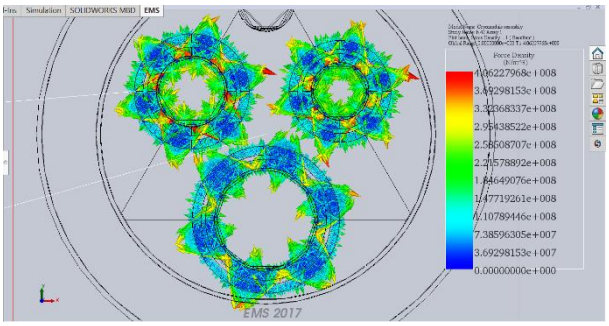

Fig. 7 Force density for Nd2Fe14B magnet (N42) and magnetic array 1

4.2 For N42 Magnet and Magnetic Array 2

Fig. *8* and Fig. *10* show the proposed model's magnetic flux density and force density with a $Nd_2Fe_{14}B$ magnet (N42) as the material having a magnetic array 2 configuration. The average magnetic flux density and force density is about 1.76×10^{-1} T and 4.65×10^{7} N/m^3, respectively. Here, all the magnetic flux lines are uniform in between the annular space of the magnetic arrays. Thus, the forces are consistent throughout the

annular space, and hence stable levitation can be confirmed.

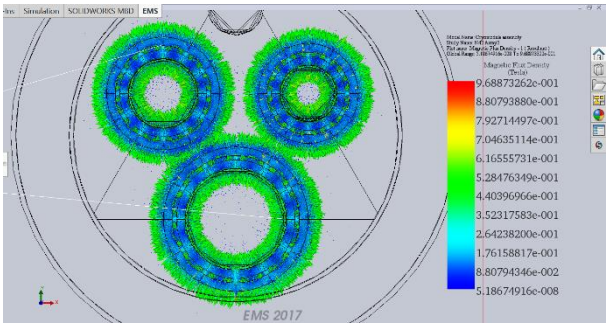

Fig. 8 Magnetic flux density for Nd2Fe14B magnet (N42) and magnetic array 2

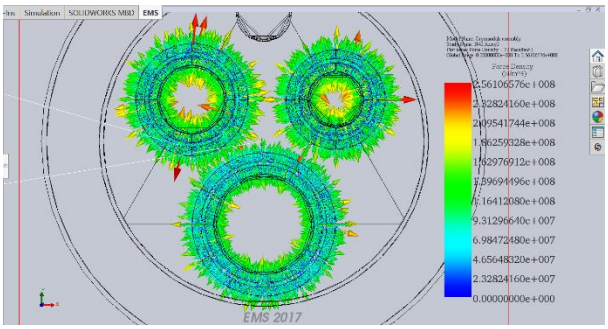

Fig. 10 Force density for Nd2Fe14B magnet (N42) and magnetic array 2

4.3 For Ceramic Magnet and Magnetic Array 1

Fig. *11* and Fig. *13* show the proposed model's magnetic flux density and force density with a ceramic magnet (grade 8) as the material having a magnetic array 1 configuration. The average magnetic flux density and force density is about 1.62×10^{-1} T and 8.39×10^{6} N/m^3,

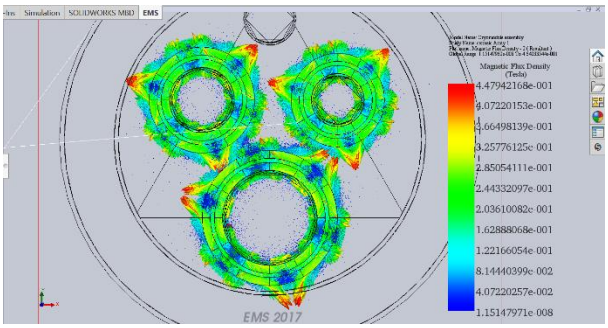

Fig. 11 Magnetic flux density for Ceramic magnet (grade 8) and magnetic array 1

respectively. As in the case $Nd_2Fe_{14}B$ magnet, there are three focus points where the flux density is highest in the annular gap between the magnetic arrays.

4.4 For Ceramic Magnet and Magnetic Array 2

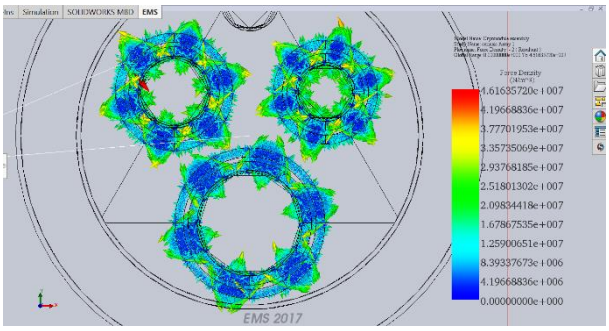

Fig. 13 Force density for Ceramic magnet (grade 8) and magnetic array 1

Fig. *12* and Fig. *9* show the proposed model's magnetic flux density and force density with a ceramic magnet (grade 8) as a material having a magnetic array 2

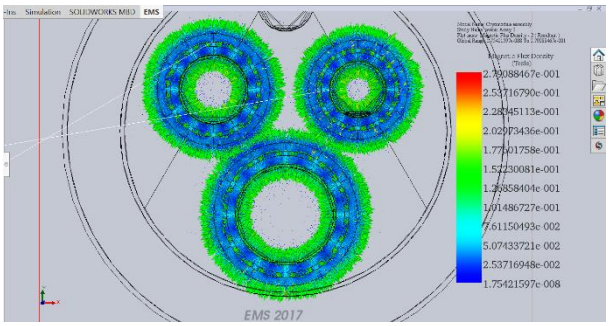

Fig. 12 Magnetic flux density for Ceramic magnet (grade 8) and magnetic array 2

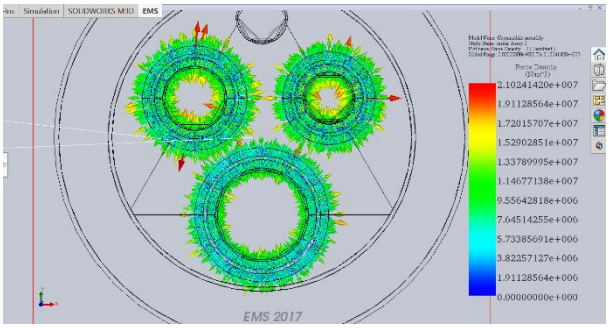

Fig. 9 Force density for Ceramic magnet (grade 8) and magnetic array 2

configuration. The average magnetic flux density and force density is about 7.61×10^{-2} T and 3.82×10^{6} N/m^3, respectively. Here, all the magnetic flux lines are uniform in between the annular space of the magnetic arrays.

5. CONCLUSION

Analysis of the results of the simulations concludes that for magnetic array 1, the magnetic field lines between the rings of the magnetic array are discrete and have three focus points; thus, the chance of rotational instability is there. But, since most magnetic field lines are in the

annular space of two magnetic arrays, the levitation's overall magnetic force is higher. Here, one can increase the number of magnets to 16 or 20 in one array to increase stability by increasing focus points. For magnetic array 2, the magnetic field lines in the annular space of two magnetic arrays are continuous and repelling each other, so that will be much more stable than the first case. However, the force density value is decreased because of magnetic field concentration both outside and inside.

For levitation of the process pipes, the required average force density value is about 6.7×10^5 N/m^3. For magnetic material $Nd_2Fe_{14}B$ (N42), the average force density value is 1.12×10^8 N/m^3 for magnetic array 1, whereas for magnetic array 2, it is 4.65×10^7 N/m^3. For magnetic material ceramic, the average force density value is 8.39×10^6 N/m^3 for magnetic array 1, while for magnetic array 2, it is 3.82×10^6 N/m^3 which is considerable. In both magnetic materials, the levitation will occur and hence could be used for levitation. Overall, by utilizing magnetic levitation, heat loss by conduction through sliding support is prevented.

REFERENCE

[1] J. G. Weisend II, *Cryostat Design*, Sweden: Springer International Publishing, Switzerland, 2016.

[2] P Duda, M Chorowski and J Polinski, "Design and thermodynamic performance analysis of multi-channel cryogenic transfer line for XFEL AMTF," *IOP Conference Series: Materials Science and Engineering, vol. 171 012043*, 2017, pp. 1-7.

[3] B. C. Deng, S. Q. Yang, X. J. Xie, Y. L. Wang, W. Pana, Q. Li and L. H. Gong, "Thermal performance assessment of cryogenic transfer line with support and multi-layer insulation for cryogenic fluid," *Applied Energy, vol. 250*, 2019, 895-903.

[4] Wikipedia Foundation, Inc., "Wikipedia," [Online]. Available: https://en.wikipedia.org/wiki/Magnetic_levitation. [Accessed 8th May 2021].

[5] Chengqian Zhang, Peng Zhao, Wen Wen, Jun Xie, Neng Xia, and Jianzhong Fu, "Density measurement via magnetic levitation: Linear relationship investigation," *Elsevier Polymer Testing, vol. 70*, 2018, 520-525,.

[6] Y.-M. Choi, Moon G. Lee, Dae-Gab Gweon and Jaehwa Jeong, "A new magnetic bearing using Halbach magnet arrays for a magnetic levitation stage," *The review of scientific Instrument, vol. 80*, 2009.

[7] Wikipedia Foundation, Inc., "Meissner Effect," Wikipedia Foundation, Inc., 3rd April 2021. [Online]. Available: https://en.wikipedia.org/wiki/Meissner_effect.

[8] Wikipedia Foundation, "Magnets," [Online]. Available: https://en.wikipedia.org/wiki/Magnet. [Accessed 31 May 2021].

[9] Solidworks, *Magnetostatic Simulation*, Solidworks, 2017.